String tension in gonihedric three-dimensional Ising models



1997 J. Phys. A: Math. Gen. 30 7695

(http://iopscience.iop.org/0305-4470/30/22/009)

J. Phys. A: Math. Gen. **30** (1997) 7695–7706. Printed in the UK PII: S0305-4470(97)82404-3

# String tension in gonihedric three-dimensional Ising models

M Baig†, D Espriu‡, D A Johnston§ and Ranasinghe P K C Malmini§‖

† IFAE, Universitat Autònoma de Barcelona, Edifici C, 08193 Bellaterra, Spain
‡ DECM and IFAE, Universitat de Barcelona, Diagonal 647, 08028 Barcelona, Spain
§ Department of Mathematics, Heriot-Watt University, Riccarton, Edinburgh EH14 4AS, UK

Received 7 March 1997

**Abstract.** For the three-dimensional gonihedric Ising models defined by Savvidy and Wegner the bare string tension is zero and the energy of a spin interface depends only on the number of bends and self-intersections, in antithesis to the standard nearest-neighbour three-dimensional Ising action. When the parameter $\kappa$, weighting the self-intersections, is small the model has a first-order transition and when it is larger the transition is continuous. In this paper we investigate the scaling of the renormalized string tension, which is entirely generated by fluctuations, using Monte Carlo simulations for $\kappa = 0.0$, 0.1, 0.5 and 1.0. The scaling of the string tension allows us to obtain an estimate for the critical exponents $\alpha$ and $\nu$ using both finite-size scaling and data collapse for the scaling function. The behaviour of the string tension when the self-avoidance parameter $\kappa$ is small also clearly demonstrates the first-order nature of the transition in this case, in contrast to larger values. Direct estimates of $\alpha$ are in good agreement with those obtained from the scaling of the string tension. We have also measured $\gamma/\nu$.

## 1. Introduction

The phase structure of Ising models with extended-range interactions in two and three dimensions is very rich in general [1, 2]. In three dimensions when the spin interfaces are regarded as describing a gas of closed surfaces one gets a similarly rich diagram for morphological transitions in an equivalent plaquette surface model [3]. The relation between the weighting of area, right-angled bends and intersections in a plaquette surface model and the couplings of an Ising model with nearest-neighbour, next-to-nearest-neighbour and plaquette interactions on the dual lattice is explicitly known [1]. This equivalence between an Ising model and a surface gas is particularly convenient for performing Monte Carlo simulations, where the Ising model transcription offers obvious practical advantages.

In this paper we are interested in a class of Ising model Hamiltonians which assign zero weight to the area of an interface. Any surface tension that appears in the model is thus generated by fluctuations. Higher spin models with zero bare surface tension [4] have been investigated in some detail, particularly in the context of wetting transitions [5], but the gonihedric Ising model realization is still relatively unexplored. The genesis of the gonihedric Ising models lies in a random surface model developed by Savvidy *et al* [6] where the action for a triangulated two-dimensional (2D) surface embedded in $\mathbb{R}^d$ is given by

$$S = \tfrac{1}{2} \sum_{\langle ij \rangle} |\boldsymbol{X}_i - \boldsymbol{X}_j| \theta(\alpha_{ij}) \tag{1}$$

‖ Permanent address: Department of Mathematics, University of Sri Jayewardenepura, Gangodawila, Sri Lanka.

0305-4470/97/227695+12$19.50  

the sum being over the edges of some triangulated surface, $\theta(\alpha_{ij}) = |\pi - \alpha_{ij}|^{\zeta}$, $\zeta$ is some exponent (smaller than 1, or else the model is ill-defined [7]), and $\alpha_{ij}$ is the dihedral angle between adjacent triangles. This action was proposed to cure some of the diseases of other triangulated random surface theories, which have proved remarkably reluctant to yield smooth continuum limits.

Taking the discretization a stage further and discretizing the target space, which thus becomes $\mathbb{Z}^d$, the authors of [8–11] rewrote the resulting theory as precisely the sort of extended Ising model considered in [1, 2]. Specializing to three dimensions, the energy of a plaquette surface in the gonihedric model is given by by $E = n_2 + 4\kappa n_4$, where $n_2$ is the number of links where two plaquettes meet at a right angle and $n_4$ is the number of links where four plaquettes meet at right angles. $\kappa$ is a free parameter which determines the relative weight of the intersections compared with the right-angled bends. The results of [1] show that an Ising Hamiltonian which gives $E = n_2 + 4\kappa n_4$ contains nearest-neighbour ($\langle i, j \rangle$), next-to-nearest-neighbour ($\langle\langle i, j \rangle\rangle$) and round a plaquette ($[i, j, k, l]$) terms

$$H = 2\kappa \sum_{\langle ij \rangle} \sigma_i \sigma_j - \frac{\kappa}{2} \sum_{\langle\langle i,j \rangle\rangle} \sigma_i \sigma_j + \frac{1-\kappa}{2} \sum_{[i,j,k,l]} \sigma_i \sigma_j \sigma_k \sigma_l. \tag{2}$$

Of course it should be pointed out that the equivalence between equations (1) and (2) is only at a very intuitive level. Ising surfaces have a degree of self-avoidance, which the gonihedric action has not. The resolution of the resulting spin configurations in terms of plaquette surfaces is also ambiguous (do the surfaces touch or cut each other?), but for large enough (additional) self-avoidance coupling $\kappa$ the distinction may be irrelevant. The ratio of coefficients that appear in equation (2) is rather particular, it corresponds to the so-called disorder variety as calculated in the mean-field approximation [12].

The above Hamiltonian displays a 'flip' symmetry—a plane of spins may be flipped with no energy cost if it does not intersect any other planes. This symmetry poses some problems in Monte Carlo simulations when one is attempting to measure, for example magnetic exponents as lamellar low-temperature configurations with arbitrary interlayer spacing render the standard magnetization

$$M = \left\langle \frac{1}{L^3} \sum_i \sigma_i \right\rangle \tag{3}$$

meaningless†. The solution adopted in [13, 14] was to fix three perpendicular planes of spins, which provided a sufficient penalty to suppress the lamellar state degeneracy and still allowed one to retain the periodic boundary conditions which minimize finite-size effects.

The phase structure of the Hamiltonian in equation (2) has been explored by both Monte Carlo [13, 14] and cluster-variational (CVPAM) methods [15, 16] with similar results: there is a single transition from a paramagnetic high-temperature phase to (with appropriate boundary conditions in the Monte Carlo case) a ferromagnetic phase. The transition point appears to be independent of $\kappa$ for $\kappa$ sufficiently large. The transition is continuous for these values of $\kappa$. The critical indices are also independent of $\kappa$. However, in the vicinity of $\kappa = 0$, where the model displays an additional 'antiferromagnetic' symmetry, the transition becomes first order [14]. A modified mean-field approach [13, 1] also predicts the same phase structure, but underestimates $\beta_c$ and gives a much stronger variation of $\beta_c$ with $\kappa$ than is seen in the simulations and CVPAM approach. In [16] it was suggested that consideration of a larger space of coupling constants for the terms in equation (2) indicated

† Although a low-temperature expansion suggests that the lamellar state actually has a slightly higher energy than the purely ferromagnetic state [15], Monte Carlo simulations with periodic boundary conditions persistently give lamellar configurations.

that the observed exponents were effective exponents arising from the proximity of the transition point to the critical endpoint of a paramagnetic–ferromagnetic line.

It was remarked by Savvidy *et al* [9] that $\beta_c$ was close to that of the standard 2D Ising model with nearest-neighbour interactions on a square lattice and the simulations in [13] found $\gamma/\nu = 1.79(4)$, close to the Onsager 2D Ising value of 1.75. These authors also found $\nu = 0.8(1)$†, not far off the 2D Ising value $\nu = 1$. However, the value of $\beta$ was estimated to be a lot smaller than the Onsager value of 0.125.

Direct and finite-size scaling fits on the specific heat data in [13] for $\alpha$ were not very reliable due to the presence of the unknown analytic part in the specific heat, which leads to an extra adjustable parameter in the fits. Part of the motivation for the current work was to obtain an alternative estimator for $\alpha$ that sidestepped these problems. Another factor was the apparent impossibility of finding discretized surface models exhibiting a proper scaling of the string tension. The ordinary three-dimensional (3D) Ising model has a scaling string tension, but it is unclear to which continuum surface model it corresponds. It is thus interesting to find equally simple models with different scaling properties, particularly if, as for the one presented here, they have a good geometrical interpretation. An additional reason to undertake this project was that, if present, the string tension in the gonihedric models should be entirely generated by fluctuations, so the simulations allow one to confirm that the standard scaling ansatz still apply in such a case. Finally, the behaviour of the string tension is an excellent indicator of a first-order transition, so a simulation at, or around, $\kappa = 0$ can confirm the first-order nature of the transition in this case. In [14] we hypothesized that the apparent impossibility of defining a continuum limit for 'ghost' surfaces ($\kappa = 0$ implies no self-avoidance) may be related to the fact that equation (1) leads to problems if $\zeta = 1$, which the Ising discretization naively corresponds to.

We now move on to discuss the measurement of the surface tension and extraction of estimates for $\alpha$ and $\nu$.

## 2. String tension

Normally when one is trying to measure a string tension in an Ising-like model it is sufficient to use antiperiodic boundary conditions in one direction because this guarantees the presence of an interface. The string tension can then be defined from the ratio of the bulk partition function $Z_0$ and the partition function with an interface $Z_I$ as

$$\sigma = \frac{1}{L^2} \log\left(\frac{Z_0}{Z_I}\right) \tag{4}$$

where we have assumed that we have a square interface spanning an $L \times L$ boundary. However, as we have seen, the gonihedric Ising models possess a symmetry which allows planes of spins to be flipped at no energy cost, so antiperiodic boundary conditions are insufficient to force an interface. Something more coercive, in the form of the fixed, or perhaps more accurately 'mixed', plus and minus spin boundary conditions shown in figure 1($a$) is necessary in order to make sure an interface exists. The fixed spins on the faces make sure that any flipped spin planes will be penalized by a boundary energy and thus discouraged. While this has the disadvantage of greater finite-size effects than antiperiodic boundaries one can also use fixed-boundary conditions in calculating the 'bulk' contribution $Z_0$, but now with all spins plus in order to eliminate the interface as shown in figure 1($b$). Since the string tension is defined from a ratio of partition functions (i.e. a difference of

† $\nu$ is inadvertently transposed with $1/\nu$ in [13].

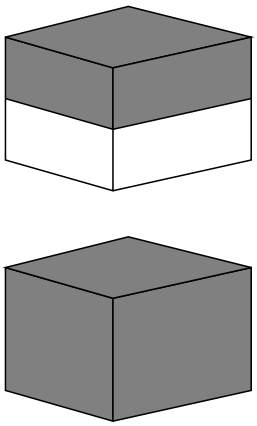

(a)

(b)

**Figure 1.** The boundary conditions used in measuring the string tension, (*a*) is used to produce an interface, (*b*) is used to ensure a ferromagnetic phase. On the shaded surfaces the spins are fixed to plus and on the white surfaces to minus.

free energies), there should be a degree of cancellation in the finite-size effects for $Z_0$ and $Z_I$.

In practice one cannot measure a partition function or free energy directly in the simulations, so one considers the derivative of the string tension with respect to $\beta$, which gives the (internal) energy difference between configurations with and without an interface

$$\frac{\partial \sigma}{\partial \beta} = \Delta E = L_z(\langle E_{++}\rangle - \langle E_{+-}\rangle) \tag{5}$$

where we have denoted the mixed boundary conditions that give the interface by $\{+-\}$ and the fixed boundary conditions by $\{++\}$ and the $\langle E\rangle$'s are energy densities. The volume of the system is $L_z \times L \times L$. If $L_z = L$, the standard finite-size scaling behaviour for the specific heat $C \sim \tilde{C}_0 + \tilde{C}_1 L^{\alpha/\nu}$ and the relation $C = \partial E/\partial\beta$ mean that one would expect

$$E \simeq E_0 + E_1 L^{\frac{\alpha-1}{\nu}} \tag{6}$$

where the constant $E_0$ has its origin in the regular term in the specific heat and would be expected to appear for both sets of boundary conditions. A measurement of the energy with a single set of boundary conditions thus gains nothing over specific heat measurements as there is still a constant term $E_0$. However, if one considers both mixed and fixed boundary conditions one would expect the *same* regular part $E_0$ for both sets. A measurement of the energy difference therefore eliminates $E_0$ and a simple power law fit to

$$\Delta E = L(\langle E_{++}\rangle - \langle E_{+-}\rangle) \propto L^{1+\frac{\alpha-1}{\nu}} = L^A \tag{7}$$

determines the exponent $A$. Similar methods have been used to extract $\alpha$ for the Heisenberg model by Holm and Janke [17].

In order to extract further estimates from our simulations we also considered the standard scaling ansatz [18] for the string tension on an asymmetric lattice. Then

$$\sigma \sim \frac{1}{L^2}\Sigma\left(tL^{1/\nu}, \frac{L_z}{L}\right) \tag{8}$$

where $t = |\beta - \beta_c|/\beta_c$. This gives directly

$$\Delta E \sim L^{-2+1/\nu}\Sigma'\left(tL^{1/\nu}, \frac{L_z}{L}\right) \tag{9}$$

so at the critical point

$$\Delta E \sim L^{-2+1/\nu}\tilde{\Sigma}'\left(\frac{L_z}{L}\right). \tag{10}$$

**Table 1.** $\Delta E/L$ for $\kappa = 1.0$, along with the estimated pseudocritical temperatures.

| $L$ | 12 | 15 | 18 | 20 | 22 | 25 |
|---|---|---|---|---|---|---|
| $\Delta E/L$ | 0.0369(28) | 0.0307(20) | 0.0281(23) | 0.0235(25) | 0.0244(21) | 0.0222(25) |
| $\beta_c(L)$ | 0.3938(4) | 0.4095(1) | 0.4124(1) | 0.4198(1) | 0.4204(1) | 0.4227(1) |

For $\kappa = 0.5$ we simulated lattices with various aspect ratios, $x = L_z/L$, and adjusted the exponent $A$ in a plot of $\Delta E\ L^{-A}$ in order to attempt to obtain a smooth scaling function $\tilde{\Sigma}'(x)$. The 'best' curve then gives an estimate of $A = -2 + 1/\nu$†. The approach can also be used on symmetric lattices away from the critical point as, referring to equation (9) when $L_z = L$, we can see that $\Delta E L^{2-1/\nu}$ plotted against $tL^{1/\nu}$ should collapse the data for various lattice sizes and temperatures to give a smooth scaling function for the correct choice of $\nu$.

## 3. Simulations

### *3.1. Energy and specific-heat exponents*

The simulations were carried out on symmetric lattices of size $10^3$, $12^3$, $15^3$, $18^3$ ,$20^3$, $22^3$ and $25^3$ for $\kappa = 1.0$. For $\kappa = 0.5$ lattices with various aspect ratios of sizes $10^2 \times 10$, $12^2 \times 10$, $14^2 \times 10$, ... $20^2 \times 10$, $16^2 \times 20$, $20^2 \times 20$, $24^2 \times 20$, and $16^2 \times 30$, $20^2 \times 30$, $24^2 \times 30$, $30^2 \times 30$ were used. Similar sizes were considered for $\kappa = 0$ and $\kappa = 0.1$. We carried out 50–1000 K measurement sweeps after allowing a suitable amount of time for thermalization, depending on the value of $\beta$ and the lattice sizes. We used the tried and tested code from [13, 14], which performs a simple metropolis update. It is worth remarking that although the gonihedric action contains competing interactions it might be worthwhile formulating a cluster update for the model as there is no frustration present. The magnetization, energy, susceptibility, specific heat and various cumulants were all measured in the standard fashion. For each lattice size we simulated separately with fixed and mixed boundary conditions in order to allow us to measure $\Delta E$ from the combined results.

Taking, for example, the $\kappa = 1.0$ results on symmetric lattices, we find that the curve of $\Delta E$ displays a maximum, which we use as our estimator for the pseudocritical point‡. The values of $\Delta E/L$ at the appropriate pseudocritical points are shown in table 1.

A fit to these values gives $\Delta E \sim L^A \sim L^{0.3(1)}$ with a $\chi^2$/degrees of freedom of 0.3. This estimate gives a much lower value for $\nu$ ($\nu = 0.44(2)$) than that in [13] which was obtained by comparison of $\gamma/\nu$ with $\gamma$ (as well as the scaling of the pseudocritical points). A plot of the scaling function for the energy in figure 2 for $\nu = 0.44$ gives quite a good collapse of the data, providing further evidence in support of this lower value.

We have only three symmetric lattice simulations to carry out a simple finite-size scaling fit for $\kappa = 0.5$, which give 0.4(1) for the exponent in the fit to $\Delta E$ versus $L$. We do have, on the other hand, a wide range of asymmetric lattice sizes on which we try out the asymmetric scaling programme outlined in section 2. In figure 3 we show a plot of $\Delta E L^{-A} = \tilde{\Sigma}'(L_z/L)$ against $L_z/L$. By inspection the smoothest data corresponds to $A \sim 0.46(4)$ which is consistent with the finite-size scaling estimate of 0.4(1) for $A$ above. Other values of $A$ are also plotted to show how the scaling curve quickly deteriorates once one moves outside the

† By hyperscaling in $D = 3$, $-2+1/\nu = 1+(\alpha-1)/\nu$, so the two definitions of $A$ we have given are equivalent.
‡ This proved more stable than using the maximum slope—i.e. maximum of the specific heat, and would in any case be expected to have the same scaling properties.

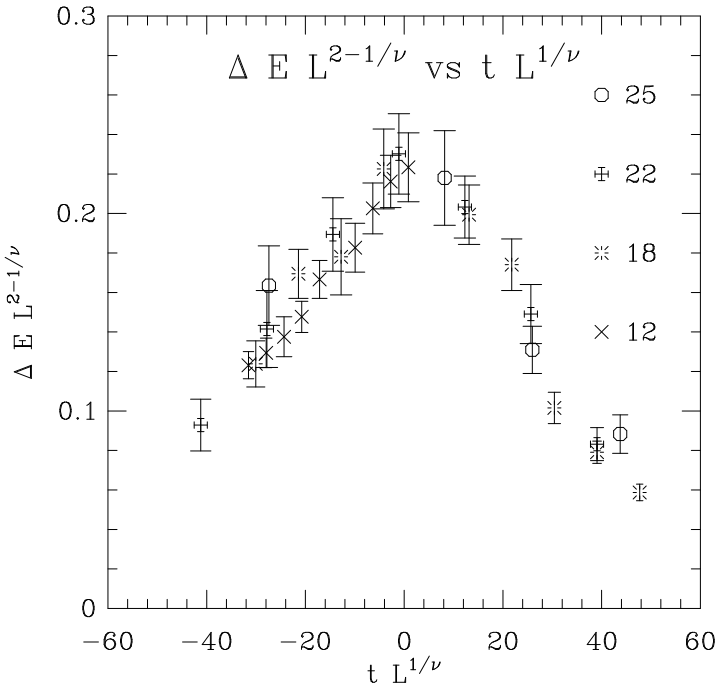


**Figure 2.** The scaling function on symmetric lattices at $\kappa = 1$, showing the good data collapse when $\nu = 0.44$. Some of the intermediate lattice sizes have been dropped for clarity.

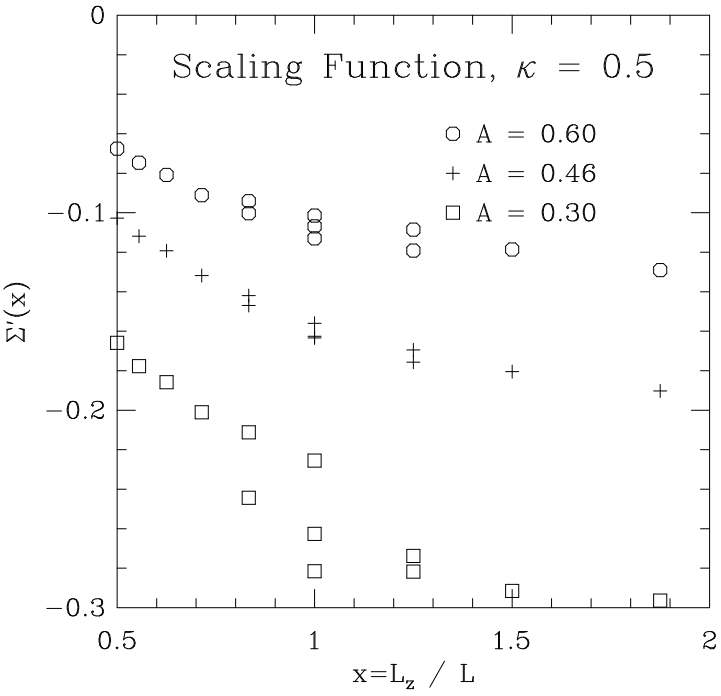


**Figure 3.** The asymmetric lattice scaling function for $\kappa = 0.5$ is plotted for various choices of the exponent $A$ defined in the text.

acceptable region for the exponent. The estimated value of $A$ for $\kappa = 0.5$ is thus somewhat higher than the value 0.3(1) obtained when $\kappa = 1.0$, but given the errors it is not possible to discern whether the exponents are different. We believe, in fact, that they are the same. In any case, the values we obtain for $A$ are clearly different from the 2D and 3D Ising model values ($A = 0$ and $A \simeq -0.4$, respectively).

It is possible to confirm that direct fits to the specific heat exponent are in agreement with the above method. Given that fits to $C \sim C_0 + C_1 t^{-\alpha}$ and $C \sim \tilde{C}_0 + \tilde{C}_1 L^{\alpha/\nu}$ are rendered untrustworthy by the presence of the analytical terms another possible approach is simply to plot $C^{-1/\alpha}$ versus $\beta$ for various choices of $\alpha$. Provided $C_0$ is not too large this would be expected to collapse all the various lattice-size data onto a straight line. This approach turns out to work remarkably well for both $\kappa = 0.5$ and $\kappa = 1.0$. In figure 4 we plot the results of the best data collapse for $\kappa = 0.5$ with $\alpha = 0.7$. Via hyperscaling, this is consistent with the estimates of $\nu$ appearing from the string tension scaling measurements. The results for $\kappa = 1.0$ are shown in figure 5. The best fit is again obtained for $\alpha = 0.7$ and the error bars can be estimated in both cases by looking at how the straight line plot deteriorates as the exponent is varied. As we have noted, standard fitting techniques for $\alpha$ are not particularly convincing with our data, but a fit to all the $\beta < \beta_c$ data for $C \sim C_0 + C_1 t^{-\alpha}$ using our best estimate of $\beta_c$ gives $\alpha = 0.5(1)$, admittedly with poor quality, for both $\kappa = 0.5$ and 1.0. In addition, the estimated value of $C_0$, while not zero, is certainly small and provides justification for the plots in figures 4 and 5. In summary, we would estimate our best fit to be $\alpha = 0.7(1)$, which supports the result obtained from the scaling of the string tension ($\nu \sim 0.44$ translates to $\alpha \sim 0.7$ with hyperscaling).

It is also worth looking at the $\kappa = 0.0$ and $\kappa = 0.1$ results for $\Delta E$ in order to see the signals of a first-order transition in the scaling of the string tension. For a first-order transition one has a finite string tension at the transition point and throughout the ordered phase. A step function in the string tension $\sigma$ translates into a delta function (centred at $\beta_c$) in the measured quantity $\Delta E$. This is precisely what is observed in the simulations both at $\kappa = 0$ itself and at small values of $\kappa$ such as 0.1 as can be seen very clearly in figure 6. Even at $\kappa = 0.1$ the sharpness of the observed peak indicates that the transition is still strongly first order.

### *3.2. Magnetic exponents*

The speculations in [13] regarding the similarity with the 2D Ising model were largely based on exponents coming from the susceptibility $\chi \sim L^{\gamma/\nu}$ and $\chi \sim t^{-\gamma}$, although it was noted that the estimate for magnetic exponent itself $M \sim L^{\beta/\nu}$, was much smaller than the Onsager 2D Ising value. It is possible to play a similar data collapse game with the susceptibility measurements to that performed with the specific heat in the previous section in order to extract an estimate for $\gamma$—one simply plots $\chi^{-1/\gamma}$ against $\beta$ for various $\gamma$ until the best straight line plot is obtained. In principle this should work even better than for the specific heat because of the absence of an analytic term in the scaling expression for the susceptibility, but the fixed and mixed boundary conditions that are imposed in the interest of obtaining an interface appear to do rather greater violence to the magnetic quantities than to the energetic ones, so the finite-size effects are large. The fixed boundary conditions give marginally better scaling behaviour than the mixed boundary conditions, so in what follows we use these. However, even in this case as a consequence of the large finite-size effects it is difficult to arrive at a precise direct determination of $\gamma$. All we can say is that it is in the region comprised between $\gamma = 1$ and $\gamma = 2$, which, admittedly, is not saying much. It is interesting that the CVPAM estimate for $\gamma$ (1.4) which is unaffected

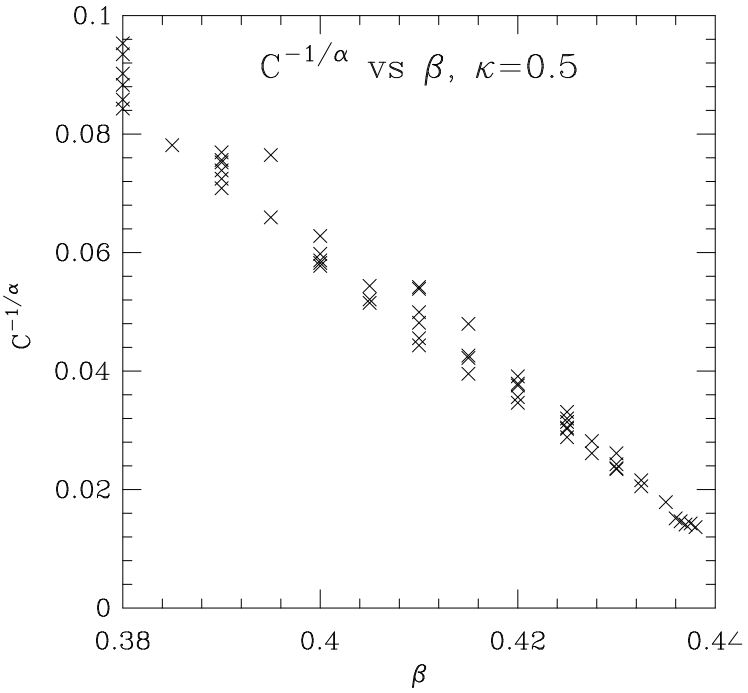


**Figure 4.** $C^{-1/\alpha}$ versus $\beta$ for the best choice of $\alpha = 0.7$ at $\kappa = 0.5$.

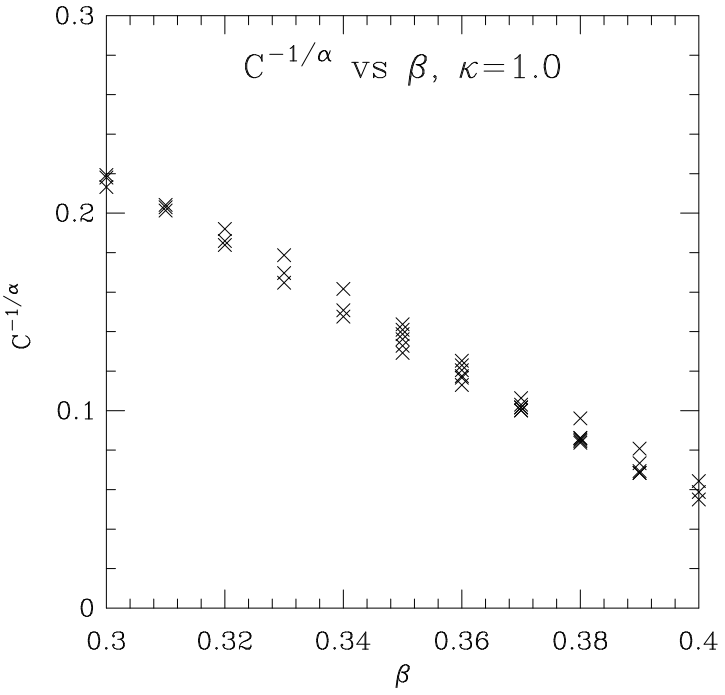


**Figure 5.** $C^{-1/\alpha}$ versus $\beta$ for the best choice of $\alpha = 0.7$ at $\kappa = 1.0$.

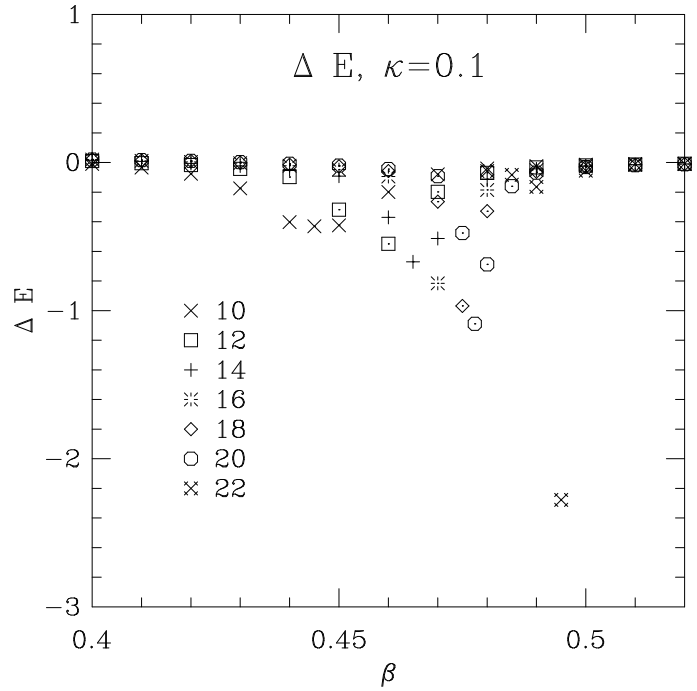


**Figure 6.** $\Delta E$ for $\kappa = 0.1$ on various asymmetric $L^2 \times 10$ lattices. The sharp peak is a clear indication of first-order behaviour.

**Table 2.** Data used in fitting $\gamma/\nu$ for $\kappa = 1.0$.

| $L$ | 12 | 15 | 18 | 20 | 22 | 25 |
|---|---|---|---|---|---|---|
| $\chi_{max}$ | 9.4(3) | 14.9(6) | 22.7(1.8) | 28.8(2.2) | 32.9(2.0) | 43.0(3.7) |
| $\beta_c(L)$ | 0.3784(3) | 0.3919(4) | 0.3975(2) | 0.4027(3) | 0.4148(1) | 0.4144(1) |

by boundary condition and finite-size considerations is also relatively small, although the systematic errors are difficult to assess in this case.

Nonetheless, finite-size scaling allows a much better measurement of $\gamma/\nu$ for both $\kappa = 0.5$ and $\kappa = 1.0$. In both cases one obtains $\gamma/\nu = 2.1(1)$. The data used in the $\kappa = 1.0$ fit on symmetric lattices is shown in table 2, which produced a fit of 2.1(1) with a $\chi^2$/degrees of freedom of 0.18.

For $\kappa = 0.5$ on asymmetric lattices we perform a finite-size scaling analysis similar to the one employed in determining the string tension scaling. We search for a universal scaling function $X(L_z/L)$ by adjusting the value of $\gamma/\nu$ in a plot of $X(L_z/L) \sim \chi L^{-\gamma/\nu}$. The smoothest function is also obtained when $\gamma/\nu = 2.05$, in excellent agreement with the $\kappa = 1$ result. The function $X$ is plotted in figure 7. To show the sensitivity of the method, we also plot $X$ for $\gamma/\nu = 1.80$ which gives a markedly less smooth curve.

A final word of warning: while the estimates obtained are rather higher than the 1.79(4) in [13] for $\gamma/\nu$ at $\kappa = 1.0$ it should be remembered that a different set of boundary conditions (periodic, with fixed *internal* spin planes) was used there, and that these might be expected to cause less severe finite-size effects for magnetic quantities. The fixed boundary conditions

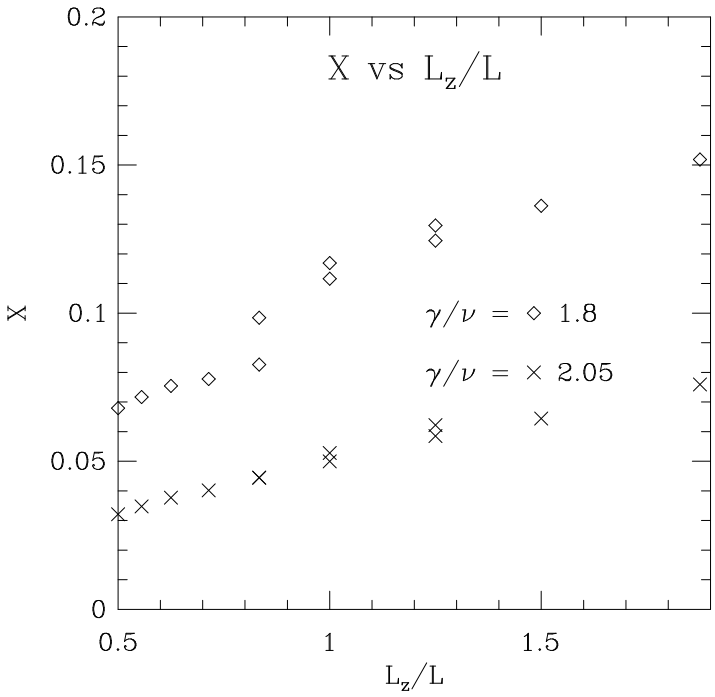


**Figure 7.** $X(L_z/L)$ for $\gamma/\nu = 1.8, 2.05$ at $\kappa = 0.5$.

are even more violent to the magnetization itself and we could obtain no reliable estimates for either the magnetization exponent $\beta$ or $\beta/\nu$ from finite-size scaling, in contrast to the periodic boundaries and fixed internal spin planes in [13].

## 4. Discussion

As we have already noted, from the results it is clear that the 2D and 3D Ising values for $A$ of 0 and $\sim -0.4$ are definitively excluded. This shows that the hypothesis floated in [13] which states that the critical behaviour of the model might be related to that of the standard 2D Ising model is not supported by the numerical evidence. There is good agreement between the various methods we have used to extract the energetic exponents ($\alpha$, $\nu$). The data collapse on both symmetric and asymmetric lattices suggests that $\alpha = 0.7(1)$ for both $\kappa = 0.5$ and 1.0 and (via both hyperscaling and directly from the data collapse) $\nu$ is in the region of 0.5. We find a value around 2 for $\gamma/\nu$ from the finite-size scaling of the susceptibility, which implies a smaller value of $\gamma$ ($\sim 1$) than that estimated in [13]. As we have noted, the estimate for $\gamma$ from the CVPAM calculations [16] is similarly small. It is also worth remarking that the estimate $\gamma/\nu \sim 2$ implies (from the Fisher scaling relation $\gamma = \nu(2-\eta)$) that the estimated value of $\eta$ is small, another indication that the critical behaviour is *not* related to the 2D Ising model. The set of exponents that we have arrived at are consistent with $\alpha + 2\beta + \gamma = 2$. In addition hyperscaling, $\alpha = 2 - \nu D$, appears to be happily satisfied by the measured values of $\alpha$ and $\nu$. The first-order nature of the transition for small $\kappa$ is also manifest in the sharp spike in the measurements of $\Delta E$ at $\beta_c$ for $\kappa = 0.0, 0.1$.

It is interesting that a similar value of $\alpha = 0.5$ appears in the vicinity of the disorder variety for the anisotropic triangular lattice Ising model [19, 20]. The Blöte and Hilhorst

transcription of the anisotropic triangular lattice Ising model as a diamond covering of the lattice is particularly intriguing from our viewpoint. In this formulation the model can be viewed as a perspective view from the (1, 1, 1) direction of a cubic lattice SOS model. The excitations in the model appear as steps, or strings of flipped diamonds in the perspective view of an otherwise flat surface. It is noteworthy that the weights which appear in their model are identical to weights for a restricted class of surface configurations in the gonihedric Ising model, namely: steps of height 1; no right-angled bends; no overhangs; and $\Delta_2$ (one of their parameters) zero. Similar $\alpha = 0.5$ singularities appear in related dimer problems [21] which can be formulated as hexagonal lattice vertex models. Indeed, it is possible to write down a vertex model that represents the full gonihedric set of surface configurations as viewed from a (1, 1, 1) perspective but this does not appear to be soluble.

Haldane and Villain [22] pointed out that a square-root singularity would be expected to appear generically in systems with string-like, or striped, excitations in two dimensions. Given the values of $\alpha$ that we have estimated from the string tension scaling here, it is not inconceivable that we have a 3D realization of these ideas in the gonihedric Ising model.

## Acknowledgments

RPKCM was supported by Commonwealth Scholarship SR0014. DE and DAJ were partially supported by EC HCM network grant ERB-CHRX-CT930343. DE acknowledges the financial support of CICYT and CIRIT through grants AEN95-0590 and GRQ93-1047, respectively. MB acknowledges the financial support of CESCA and the financial support of CICYT through grant AEN95-0882. DAJ would like to thank Wolfhard Janke for clarifying discussions on the scaling form of $\Delta E$. DE would like to thank the hospitality of the CERN TH Division where this work was finished.

## References

[1] Cappi A, Colangelo P, Gonella G and Maritan A 1992 *Nucl. Phys.* B **370** 659
[2] Selke W 1988 *Phys. Rep.* **170** 213
Landau D P and Binder K 1985 *Phys. Rev.* B **31** 5946
[3] Sterling T and Greensite J 1983 *Phys. Lett.* **121B** 345
Karowski M and Thun H 1985 *Phys. Rev. Lett.* **54** 2556
Karowski M 1986 *J. Phys. A: Math. Gen.* **19** 3375
[4] Schmid F and Schick M 1994 *Phys. Rev.* E **49** 494
[5] Dietrich S 1989 *Phase Transitions and Critical Phenomena* vol 13, ed C Domb and J L Lebowitz (London: Academic)
[6] Ambartzumian R V, Sukiasian G S, Savvidy G K and Savvidy K G 1992 *Phys. Lett.* B **275** 99
Savvidy G K and Savvidy K G 1993 *Int. J. Mod. Phys.* A **8** 3393
Savvidy G K and Savvidy K G 1993 *Mod. Phys. Lett.* A **8** 2963
[7] Durhuus B and Jonsson T 1992 *Phys. Lett.* B **297** 271
[8] Savvidy G K and Wegner F J 1994 *Nucl. Phys.* B **413** 605
Savvidy G K and Savvidy K G 1994 *Phys. Lett.* B **324** 72
Savvidy G K, Savvidy K G and Savvidy P G 1996 *Phys. Lett.* A **221** 233
Savvidy G K and Savvidy K G 1994 *Phys. Lett.* B **337** 333
Savvidy G K, Savvidy K G and Wegner F J 1995 *Nucl. Phys.* B **443** 565
[9] Bathas G K, Floratos K G, Savvidy G K and Savvidy K G 1995 *Mod. Phys. Lett.* A **10** 2695
[10] Savvidy G K and Savvidy K G 1996 *Mod. Phys. Lett.* A **11** 1379
[11] Pietig R and Wegner F 1996 *Nucl. Phys.* B **466** 513
[12] Gonella G, Lise S and Maritan A 1995 *Europhys. Lett.* **32** 735
[13] Johnston D A and Malmini R K P C 1996 *Phys. Lett.* B **378** 87
[14] Baig M, Espriu D, Johnston D A and Malmini R K P C 1997 *J. Phys. A: Math. Gen.* **30** 405
[15] Cirillo E, Gonnella G, Pelizzola A and Johnston D 1997 *Phys. Lett.* A **226** 59

[16] Cirillo E, Gonnella G and Pelizzola A 1997 New critical behaviour of the three dimensional Ising model with nearest neighbour, next nearest neighbour and plaquette interactions *Phys. Rev.* E to appear
[17] Holm C and Janke W 1994 *J. Phys. A: Math. Gen.* **27** 2553
[18] Privman V 1990 *Finite Size Scaling and Numerical Simulation of Statistical Systems* (Singapore: World Scientific)
[19] Blöte H and Hilhorst H 1982 *J. Phys. A: Math. Gen.* **15** L631
[20] Georges A, Hansel D, Le Doussal P and Maillard J 1986 *J. Phys. A: Math. Gen.* **19** L329
[21] Wu F 1968 *Phys. Rev.* **168** 539
[22] Haldane F and Villain J 1981 *J. Physique* **42** 1673